Fossil eggshell cuticle elucidates dinosaur nesting ecology

Tzu-Ruei Yang [Corresp., 1] , Ying-Hsuan Chen [2] , Jasmina Wiemann [3] , Beate Spiering [4] , P. Martin Sander [5, 6]

[1] Bereich Paläontologie, Steinmann-Institut für Geologie, Mineralogie und Paläontologie, Universität Bonn, Bonn, Germany

[2] Max-Planck-Institut für Eisenforschung, Düsseldorf, Germany

[3] Department of Geology and Geophysics, Yale University, New Haven, Connecticut, United States

[4] Bereich Mineralogie, Steinmann-Institut für Geologie, Mineralogie und Paläontologie, Rheinische Friedrich-Wilhelms Universität Bonn, Bonn, Germany

[5] Bereich Paläontologie, Steinmann-Institut für Geologie, Mineralogie and Paläontologie, Universität Bonn, Bonn, Germany

[6] Dinosaur Institute, Natural History Museum of Los Angeles County, Los Angeles, California, United States of America

Corresponding Author: Tzu-Ruei Yang
Email address: tryang@uni-bonn.de

The cuticle layer consisting mainly of lipids and hydroxyapatite (HAp) atop the mineralized avian eggshell is a protective structure that prevents the egg from dehydration and microbial invasions. Previous ornithological studies have revealed that the cuticle layer is also involved in modulating the reflectance of eggshells in addition to pigments (protoporphyrin and biliverdin). Thus, the cuticle layer represents a crucial trait that delivers ecological signals. While present in most modern birds, direct evidence for cuticle preservation in stem birds and non-avian dinosaurs is yet missing. Here we present the first direct and chemical evidence for the preservation of the cuticle layer on dinosaur eggshells. We analyze several theropod eggshells from various localities, including oviraptorid *Macroolithus yaotunensis* eggshells from the Late Cretaceous deposits of Henan, Jiangxi, and Guangdong in China and alvarezsaurid *Triprismatoolithus* eggshell from the Two Medicine Formation of Montana, United States, with the scanning electron microscope (SEM), electron probe micro-analysis (EPMA), and Raman spectroscopy (RS). The elemental analysis with EPMA shows high concentration of phosphorus at the boundary between the eggshell and sediment, representing the hydroxyapatitic cuticle layer (HAp). Depletion of phosphorus in sediment excludes the allochthonous origin of the phosphorus in these eggshells. The chemometric analysis of Raman spectra collected from fossil and extant eggs provides further supportive evidence for the cuticle preservation in oviraptorid and probable alvarezsaurid eggshells. In accordance with our previous discovery of pigments preserved in Cretaceous oviraptorid dinosaur eggshells, we validate the cuticle preservation on dinosaur eggshells through deep time and offer a yet unexplored resource for chemical studies targeting the evolution of dinosaur nesting ecology. Our study also suggests that the cuticle structure can be traced far back to maniraptoran dinosaurs and enhance their reproductive success in a warm and mesic

habitat such as Montana and southern China during the Late Cretaceous.

1   **Fossil eggshell cuticle elucidates dinosaur nesting ecology**

3   Tzu-Ruei Yang[1]*, Ying-Hsuan Chen[2], Jasmina Wiemann[3], Beate Spiering[4], P. Martin Sander[1,5]
4
5   [1]Bereich Paläontologie, Steinmann-Institut für Geologie, Mineralogie und Paläontologie,
6   Universität Bonn, Nußallee 8, 53115 Bonn, Germany
7   [2]Max-Planck-Institut für Eisenforschung, Max-Planck-Straße 1, 40237 Düsseldorf, Germany
8   [3]Department of Geology and Geophysics, Yale University, 06511 New Haven, CT, U.S.A.
9   [4]Bereich Mineralogie, Steinmann-Institut für Geologie, Mineralogie und Paläontologie,
10   Universität Bonn, Poppelsdorfer Schloss, 53115 Bonn, Germany
11   [5]Dinosaur Institute, Natural History Museum of Los Angeles County, 900 Exposition Boulevard,
12   Los Angeles, CA 90007, USA
13
14   Corresponding author:
15   Tzu-Ruei Yang[1]
16
17   Email address: tryang@uni-bonn.de or lereage@gmail.com

18 **Abstract**
19 The cuticle layer consisting mainly of lipids and hydroxyapatite (HAp) atop the mineralized
20 avian eggshell is a protective structure that prevents the egg from dehydration and microbial
21 invasions. Previous ornithological studies have revealed that the cuticle layer is also involved in
22 modulating the reflectance of eggshells in addition to pigments (protoporphyrin and biliverdin).
23 Thus, the cuticle layer represents a crucial trait that delivers ecological signals. While present in
24 most modern birds, direct evidence for cuticle preservation in stem birds and non-avian
25 dinosaurs is yet missing. Here we present the first direct and chemical evidence for the
26 preservation of the cuticle layer on dinosaur eggshells. We analyze several theropod eggshells
27 from various localities, including oviraptorid *Macroolithus yaotunensis* eggshells from the Late
28 Cretaceous deposits of Henan, Jiangxi, and Guangdong in China and alvarezsaurid
29 *Triprismatoolithus* eggshell from the Two Medicine Formation of Montana, United States, with
30 the scanning electron microscope (SEM), electron probe micro-analysis (EPMA), and Raman
31 spectroscopy (RS). The elemental analysis with EPMA shows high concentration of phosphorus
32 at the boundary between the eggshell and sediment, representing the hydroxyapatitic cuticle
33 layer (HAp). Depletion of phosphorus in sediment excludes the allochthonous origin of the
34 phosphorus in these eggshells. The chemometric analysis of Raman spectra collected from fossil
35 and extant eggs provides further supportive evidence for the cuticle preservation in oviraptorid
36 and probable alvarezsaurid eggshells. In accordance with our previous discovery of pigments
37 preserved in Cretaceous oviraptorid dinosaur eggshells, we validate the cuticle preservation on
38 dinosaur eggshells through deep time and offer a yet unexplored resource for chemical studies
39 targeting the evolution of dinosaur nesting ecology. Our study also suggests that the cuticle
40 structure can be traced far back to maniraptoran dinosaurs and enhance their reproductive
41 success in a warm and mesic habitat such as Montana and southern China during the Late
42 Cretaceous.

Introduction
Cuticle structures and functions

An avian egg is an evolutionary invention that protects the developing embryo against mechanical damage, dehydration, and microbial invasion (Romanoff & Romanoff, 1949; Board & Fuller, 1974). This multi-functionality is contributed to by both mineralized and non-mineralized organic layers, which exhibit unique biomaterial properties. The avian eggshell forms inside the uterus. The final layer to be deposited, the eggshell cuticle, represents the interface between the embryo inside and its outside environment. Many bird eggs are equipped with a cuticle layer; however, this structure is absent in some clades such as parrots, petrels, and pigeons (D'Alba et al., 2016). The cuticle layer is often described as "waxy" due to its high amount of lipids, which keep the internal fluids from evaporating and therefore protect the encased embryo from desiccation. In addition to lipids, the avian cuticle contains proteins, polysaccharides, calcium carbonate (vaterite), calcium phosphates (hydroxyapatite, HAp), and pigments (Wedral et al., 1974; Nys et al., 1991; Packard & DeMarco, 1991; Dennis et al., 1996; Mikhailov & Ornithologists' Club, 1997; Fraser, Bain & Solomon, 1999; Cusack, Fraser & Stachel, 2003; Igic et al., 2015).

The cuticle layer varies in thickness (up to 12μm) and has a patchy distribution on the eggshell (Board & Halls, 1973). Basically, the cuticle is divided into two distinct layers, including an amorphous HAp/vaterite inner layer and a proteinaceous outer layer (Simons, 1971; Dennis et al., 1996; Fraser, Bain & Solomon, 1999). The inner cuticle layer is composed of needle-like HAp/vaterite crystals on some avian eggs but present in the form of nanospherical HAp/vaterite on other avian eggs (Dennis et al., 1996; D'Alba et al., 2014). A recent study suggested that the circular mineral nanospheres on eggshells serve an antimicrobial function for species nesting in humid environment (D'Alba et al., 2016). D'Alba et al. (2016) also proposed that eggs in humid environments tend to have more cuticular nanospheres to prevent flooding and microbial invasions. Conversely, in arid environments, lacking a cuticle layer would be beneficial for embryos in eggs with low conductance, as Deeming (1987) suggested. However, in an extreme environment such as the Antarctic, Adélie penguin eggs have a thick cuticle layer to reduce water loss (Thompson & Goldie, 1990). Besides, the intactness of the cuticle is an indicator for the freshness of an egg (Rodríguez-Navarro et al., 2013). Several studies suggested that the cuticle functions as a lubricant that facilitates egg rotation in the uterus (Rahman et al., 2009). Moreover, a recent study shows that the cuticle also modulates ultraviolet reflectance of avian eggshells (Fecheyr-Lippens et al., 2015). For instance, an extremely smooth cuticle produces glossiness and iridescence in tinamou eggs (Igic et al., 2015).

The cuticle is commonly observed on most calcified eggshells, but it shows different structures and characteristics between reptilian and avian eggshells (Ferguson, 1982). The cuticle on reptilian eggshells is no longer present after two weeks of laying (Ferguson, 1982); hence, the author concluded that the reptilian cuticle is not equivalent to the cuticle present on avian eggshells. Ferguson (1982) hypothesized that a true cuticle layer is not present on alligator eggshell. Conversely, avian eggshells exhibit an inner cuticle layer composed of HAp/vaterite granules or amorphous needle-like HAp/vaterite crystals, which are absent on reptilian eggshells. Several studies on extant eggshell have identified cuticle presence by means of the scanning electron microscopy (SEM) and transmission electron microscopy (TEM) (Fink et al., 1993; Fraser, Bain & Solomon, 1999). Kusada et al. (2011) used energy dispersive X-ray analysis (EDX) to map the phosphorus (P) and calcium (Ca) distribution in several extant avian eggshells and discovered that P is confined to the cuticle layer. Although the P concentration in the cuticle

89   varies greatly between different bird species, P is a distinct marker for identifying the cuticle
90   layer in case of P depletion in sediment. Although it is still not clear how P functions during the
91   eggshell formation, a study suggested that the inclusion of P in the biomineral terminates
92   eggshell growth since it competes with calcium during the eggshell crystallization (Cusack,
93   Fraser & Stachel, 2003).
94

Discoveries of fossilized organic membranes

96   Since the cuticle is composed of proteins, polysaccharides, lipids, calcium carbonate,
97   calcium phosphates, and pigments, it is seemingly unlikely to preserve during the fossilization
98   process. A previous report concerning spherical (*Oölithus spheroides*) and elongated (*Oölithus*
99   *elongatus*) eggs from Laiyang, Shandong, China, suggested that the cuticle is preserved in
100   elongated eggs but not in spherical ones (Chow, 1954). Another similar report on ornithoid
101   eggshells from Naran-Bulak, Mongolia also described possible cuticle preservations (Sochava,
102   1971), but no diagnostic chemical data were obtained. Kohring & Hirsch (1996) studied the
103   crocodilian and ornithoid eggshells from the middle Eocene of the Geiseltal, Germany, and
104   suggested possible cuticle and shell membrane preservation. Later, with the SEM, several studies
105   on dinosaur eggshells, Cretaceous bird eggshells, and fossil moa eggshells showed the potential
106   of cuticle preservation (Mikhailov, 1991; Varricchio & Jackson, 2004; Jackson & Varricchio,
107   2010; Oskam et al., 2010). Although these studies provided a new avenue to understanding soft-
108   part preservation, all previous studies described possible cuticle preservation only based on
109   micro-structural comparisons with the cuticle of extant avian eggshells. Jackson and Varricchio
110   (2010) described a new ootaxon – *Triprismatoolithus stephensi* – of probable alvarezsaurid
111   affinities. These authors reported a cracked and amorphous surface overlying the external layer
112   and suggested it might be a layer of cuticle. Nevertheless, they did not further investigate the
113   possible cuticle layer by means of any other analyses. Therefore, all previous reports regarding
114   the cuticle preservation were constrained to micro-morphological observations. The only
115   chemical evidence supporting the fossilization potential of cuticle through deep time is offered
116   by a study on oviraptorid eggshells focusing on the two main eggshell pigments, biliverdin and
117   protoporphyrin (Wiemann et al., 2017). The protoporphyrin is deposited predominantly in the
118   cuticle layer (Schwartz et al., 1975; Nys et al., 1991; Mikšík et al., 2007; Nys & Guyot, 2011),
119   thus providing indirect evidence of cuticle preservation in the preservation of endogenous
120   protoporphyrin (Wiemann et al., 2017). Although Wilson et al. (2017) demonstrated that there is
121   no codependence of the deposition of pigment and cuticle, the preserved pigments in the
122   oviraptorid eggshell could derive from the eggshell or the preserved cuticle layer and in the latter
123   instance would be indicative of cuticle preservation. We hence posited that the cuticle was
124   completely, or partially, preserved on the oviraptorid eggshells. In addition to the cuticle layer,
125   the *membrana testacea* (eggshell membranes), a proteinaceous meshwork that underlies the
126   mineralized eggshell and separates egg yolk and eggshell, is also a crucial membrane. Unlike the
127   cuticle layer, the preservation of *membrana testacea* has been reported from titanosaurid and
128   *Lufengosaurus* eggs (Grellet-Tinner et al., 2005; Reisz et al., 2013), yet never in theropod eggs.
129

Nesting ecology of dinosaurs and modern birds

131   Dinosaur nesting ecology is a long-standing and intriguing research topic. Among all
132   dinosaurs, the nesting type of titanosaur, troodontid, and oviraptorid dinosaurs are comparatively
133   well documented (Jackson et al., 2007; Varricchio et al., 2013; Wiemann et al., 2017). These
134   dinosaurs adopted different nesting strategies in their clutch arrangement, nest architecture, and

135 nesting mode. Deeming (2006) and Tanaka, Zelenitsky & Therrien (2015) roughly categorized
136 two nesting modes in dinosaurs, including open and buried nesting modes. Most birds build open
137 nests, while the buried nesting mode is only observed in megapode birds. In a wet incubation
138 environment such as a buried megapode nest, eggs are exposed to a higher risk of asphyxiation
139 and microbial infection (Board & Fuller, 1974; Board, 1982; D'Alba et al., 2017). D'Alba et al.
140 (2016) provided the first report regarding the association between the cuticular nanospheres and
141 nesting modes. These authors discovered that the birds nesting in more mesic environments tend
142 to lay eggs yielding cuticular nanospheres. The nanospheres in the cuticle layer, therefore,
143 represents a structural adaptation that prevents eggs from microbial invasions (D'Alba et al.,
144 2016). However, eggs of Adélie penguins are also encapsulated by a thick cuticle layer that
145 prevents eggs from water loss in the severe cold Antarctic environment (Thompson & Goldie,
146 1990). These lines of evidence suggest that the cuticle layer is an evolutionarily labile structure
147 and thus varies greatly in accordance with the nesting environment. D'Alba et al. (2016) further
148 suggested that cuticular nanospheres are an ancestral trait; however, this trait has been lost
149 multiple times and is absent in some avian clades.
150   In dinosaurs, it was suggested that titanosaurs also employed the buried nesting mode
151 (Sander et al., 1998; Grellet-Tinner & Fiorelli, 2010; Sander et al., 2008; Vila et al., 2010;
152 Hechenleitner, Grellet-Tinner & Fiorelli, 2015). The low porosity of titanosaur eggs from Auca
153 Mahuevo, however, suggested that the titanosaurs from Auca Mahuevo did not bury their eggs
154 (Jackson, 2007; Sander et al., 2008). The Auca Mahuevo exception demonstrates that the
155 eggshell is a labile structure, which alters according to the environment. In comparison with the
156 well-documented titanosaur nesting ecology, the nesting ecology of theropods has remained
157 uncertain until recent times. A nesting *Nemegtomaia* discovered in Mongolia indicated a semi-
158 open nesting mode based on sedimentological evidence (Fanti, Currie & Demchig, 2012). The
159 discovery of pigmentation in oviraptorid eggshells strongly suggested that the oviraptorid eggs
160 were laid in an at least partially open nest (Wiemann et al., 2017). Yang et al. (2015, see also
161 Wiemann et al., 2017) further supported the semi-open nesting mode according to the
162 heterogeneous distribution of porosity in an oviraptorid egg and taphonomic evidence. While
163 there is no evidence of pigmentation in troodontid eggshells because these have not been
164 analyzed chemically so far, the heterogeneous distribution of porosity suggests that the
165 troodontid dinosaurs might also have laid their eggs in a semi-open nest (Varricchio et al., 1997;
166 Varricchio et al., 2013).
167   The goal of this study is to present further evidence of cuticle preservation on dinosaur
168 eggshells by means of SEM imaging, elemental analysis, and RS. In particular, we analyzed
169 theropod eggshells from the Nanxiong Group in China and the Two Medicine Formation in
170 Montana, USA. Both the Nanxiong Group and Two Medicine Formation represent fluvial
171 deposits, indicating a probable humid climate in both areas during the Late Cretaceous. In
172 addition, nesting on the ground or in a mound in a wet environment increases the risk of
173 microbial invasions (D'Alba et al., 2016), a cuticle layer should thus be prevalent on eggshells of
174 ground nesting theropods in a humid climate.
175
176 **Material and methods**
177   *Materials*
178   In order to standardize our following analyses, domestic chicken eggshell (*Gallus gallus*
179 *domesticus*) was obtained from a commercial source (supermarket). Two extant crocodilian
180 eggshells (*Crocodylus porosus* and *Tomistoma schlegelii*) were sampled from the collection of

181   the NMNS as negative controls (Table 1). The fossil materials include oviraptorid and probable
182   alvarezsaurid dinosaur eggshells (Table 1).
183   We studied three oviraptorid eggshell specimens that were collected from the Late
184   Cretaceous Nanxiong Group of three localities in China (Henan Province, Jiangxi Province, and
185   Guangdong Province) and are housed at the NMNS and STIPB. Based on eggshell
186   microstructure, all specimens were assignable to *Macroolithus yaotunensis*, which was laid by
187   the oviraptorid *Heyuannia huangi* (Cheng et al., 2008). *Macroolithus yaotunensis* is
188   characterized by an undulating boundary between two crystalline layers, i.e., the outer prismatic
189   layer and the inner mammillary layer (Supplemental Information; Zhao, 1975). The first
190   *Macroolithus yaotunensis* eggshell was taken from specimen NMNS CYN-2004-DINO-05-I,
191   which was collected from the Late Cretaceous Tangbian Formation of the Hongcheng Basin in
192   Jiangxi Province, China (Table 1). The Tangbian Formation is characterized by fine-grained
193   brownish-reddish sediments with dispersed coarse clasts and conglomerates, representing a
194   fluvial/alluvial environment with occasional stream flooding during the Campanian stage (Chen
195   et al., 2017). The second *Macroolithus yaotunensis* sample was collected as isolated shell
196   fragments from the Late Cretaceous Hugang Formation in the Liguanqiao Basin near Nanyang,
197   southwestern Henan Province, China (Table 1). This sample has been housed in STIPB since
198   1985 and was described in Erben (1995). The Hugang Formation is composed of dark grayish
199   red breccia with interbeds of calcareous sandstone, indicating a fluvial/alluvial environment
200   (Zhang, 2009). The third *Macroolithus yaotunensis* sample was also obtained as isolated shell
201   fragments from the Late Cretaceous fluvial deposits of the Pingling Section of the Shanghu
202   Formation in the Nanxiong Basin, located in the northwestern part of Guangdong Province,
203   China (Table 1). The NE-SW striking Nanxiong Basin, which is filled with dark purplish silty
204   mudstone with interbeds of conglomerate, has produced numerous theropod egg clutches and
205   eggshell fragments (Erben, 1995).
206   The *Triprismatoolithus stephensi* eggshells (MOR ES101), probably attributable to
207   alvarezsaurids (Agnolin et al., 2012; Varricchio & Jackson, 2016), were collected as isolated
208   shell fragments in the lower portion of the Two Medicine Formation in the Sevenmile Hill
209   outcrops, Teton County, Montana, USA (Table 1). The *Triprismatoolithus stephensi* eggshell has
210   three crystalline layers, including an external layer, prismatic layer, and mammillary layer, from
211   outermost to innermost (Varricchio & Jackson, 2016). The Two Medicine Formation is mostly
212   composed of sandstone, deposited by rivers and deltas on the western shoreline of the Late
213   Cretaceous Interior Seaway.
214
215   *Chemical analyses*
216   For the chemical analyses, we first used a VEGA TS5130 LM (Tescan) SEM at the STIPB
217   to locate and image plausible cuticle preservation on the studied eggshells. The eggshells were
218   naturally broken fragments and coated with gold for SEM observation. The operating conditions
219   for the SEM were set as 20 kV accelerating voltage.
220   All samples were cleaned with ethanol before chemical analyses. We then performed
221   elemental analyses using the EPMA equipped with a WDS at the Section of Mineralogy of the
222   STIPB to elucidate the P distribution in the radial section of dinosaur eggshells. All samples
223   were polished, fixed on a glass slide with araldite histological resin, and then coated with carbon
224   for the elemental analysis with EPMA. The elemental analyses were performed with a JEOL
225   SUPERPROBE 8900 EPMA at the same lab. The operating conditions for the EPMA were set as
226   1 μm beam diameter, 15 kV accelerating voltage, and 15 nA specimen current. The ZAF

227   correction scheme was used. Natural and synthetic minerals were used as standards.
228   We performed two rounds of RS using two Raman spectrometers at the **MPIE**. For the first
229   round, Raman Analysis I (referred to as RI hereafter)), we analyzed the domestic chicken
230   eggshell from a commercial source with a WITec Alpha300 system with 532 nm wavelength
231   laser light and a confocal 50x objective, each for 20 seconds. Since the cuticle on the chicken
232   eggshell was easily identified with the naked eye, as well as under the SEM (Figs. 1C & 1D), the
233   first round confirmed the detectability by Raman spectroscopy of the HAp of the cuticle layer
234   (Figs. 1E-F). Due to the incomplete preservation of the cuticle in the chicken eggshell, we
235   performed Raman surface mapping on the area where we found possible cuticle remains using
236   the SEM and EPMA previously.
237   Raman analysis II (referred to as RII hereafter) was performed using the Horiba Jobin Yvon
238   GmbH LabRam Raman spectrometer equipped with a 632 nm laser. All results were obtained
239   using the 10x objective of the integrated Olympus microscope. While the 10x objective is not
240   strongly sensitive to rare compounds, it provides a larger field of view for faster qualitative
241   detection of HAp on eggshell sample than in RI. In order to distinguish HAp and calcite from
242   sediments, we collected Raman spectra of the fresh chicken eggshell, the studied fossil eggshells
243   and their associated sediments (Fig. 2A). All Raman spectra of eggshells and their associated
244   sediments during RII were imported into the statistics software R and normalized with the R
245   package "ChemoSpec" (Hanson, 2017). We performed principle component analysis (PCA) on
246   the spectral area of 500 to 1500 cm^{-1} using the same package (Fig. 2B).
247
248   **Results**
249   The cuticle layer on the *Gallus* eggshell was easily observed with the naked eye. The RI
250   Raman spectrum from the *Gallus* eggshell shows a significant peak at 1087 cm^{-1} that arises from
251   the calcite, which is the major component of eggshell (Fig. 1F). Another intense peak at 967 cm^{-1}
252   was assigned to the v_3 symmetric stretching vibrations (Walters et al., 1990; Gergely et al., 2010;
253   Frost et al., 2014; Igic et al., 2015). Targeting the 967 cm^{-1} peak, the Raman surface scan shows
254   the patchy distribution of the HAp layer overlying the calcitic eggshell (Fig. 1E). The result
255   demonstrates detectability of the inner HAp layer of the cuticle by RS.
256   On the outside of *Macroolithus yaotunensis* and *Triprismatoolithus stephensi* eggshell
257   fragments, we also found peaks in these spectral regions (Fig. 2A). RII showed two intense broad
258   peaks that are located between 1063-1097 cm^{-1} and 972-986 cm^{-1} in the spectra. The spectral
259   range of 1063-1097 cm^{-1} can be assigned to the C-O bond of calcite, which is observable in the
260   spectra from all eggshells. The 972-986 cm^{-1} spectral ranges arose possibly from the phosphate (
261   PO_4^{3-}) or hydrogen phosphate (HPO_4^{2-}) (Sauer et al., 1994; Crane et al., 2006; Igic et al., 2015).
262   Importantly, the 972-986 cm^{-1} spectral ranges are present in the spectra from the chicken and
263   dinosaur eggshells but absent in the ones from the crocodilian eggshells and surrounding
264   sediments. The chemometric analysis using ChemoSpec suggests that both chicken and dinosaur
265   eggshells show similar spectral pattern between 800 cm^{-1} and 1200 cm^{-1} (Fig. 2B). In addition,
266   the spectra from the crocodilian eggshells and surrounding sediments occupy different
267   chemospaces from the ones of dinosaur and chicken eggshells (Fig. 2B).
268   Under the polarizing microscope, the *Macroolithus* eggshell from the Hongcheng Basin of
269   Jiangxi, China, displayed distinct two crystalline layers overlain by an enigmatic layer and
270   surrounding sediment (Fig. 3A). These features are also present in the other two *Macroolithus*
271   eggshells (see Supplemental Information). The uneven thickness of the prismatic layer in the
272   Jiangxi *Macroolithus* eggshells was a result of unpolished natural fracture surface of the section

273   (Fig. 3B). A possible patchy and flake-like cuticle layer was observed with SEM on the outer
274   surface of the *Macroolithus* and *Triprismatoolithus* eggshells (Figs. 3C & 4B). Furthermore, an
275   enigmatic protruding fiber-like structure was recognized in the *Triprismatoolithus* eggshell (Figs.
276   4C-D). The diameter of the fiber-like structure is approximately 3 μm.
277   We performed ten elemental line-mappings on each eggshell with EPMA and targeted
278   phosphorus of the HAp. Of the of total 30 line mappings on the three *Macroolithus yaotunensis*
279   eggshell, only two of them, which were from the Jiangxi and Guangdong specimens, show a
280   significant phosphorus peak on the boundary between the eggshell and surrounding sediment
281   (Figs. 3D & 3F). The elemental analysis also indicates the scarcity of the phosphorus in the
282   surrounding sediment. In addition, the P concentration increases from the mammillary layer to
283   the prismatic layer in all analyzed oviraptorid eggshells (Figs. 3D-F and raw data in the
284   Supplemental Information).
285   In the EPMA line-scan on the *Triprismatoolithus stephensi* eggshell, three significant peaks
286   for P were observed (Fig. 4E). The peak on the boundary between the eggshell and surrounding
287   sediment indicates possible cuticle preservation (Fig. 4E). However, the other two peaks were
288   seen in the sediment and on the boundary between the external layer and prismatic layer. The
289   variation of P concentration between different eggshell layers was also observed in
290   *Triprismatoolithus stephensi* eggshell (Fig. 4E and Supplemental Information). Although the P
291   concentration within the mammillary and prismatic layers shows little variation, the external
292   layer has a significantly lower concentration of P than the mammillary and prismatic layers (Fig.
293   4E & raw data in the Supplemental Information).
294
295   **Discussion**
296   *Elemental analysis of theropod eggshells*
297   While previous studies have reported possible preservation of cuticle and *membrana*
298   *testacea* (Chow, 1954; Kohring & Hirsch, 1996; Grellet-Tinner, 2005; Jackson & Varricchio,
299   2010; Reisz et al., 2013; Yang et al., 2015), none of these studies employed chemical analyses to
300   test this hypothesis. In this study, elemental analysis suggests the preservation of the inner
301   hydroxyapatitic cuticle layer based on the high concentration of P at the boundary between
302   eggshell and sediment. However, the peak that corresponds to a high concentration of P is not
303   always present in each elemental line-scan. For instance, on the *M. yaotunensis* eggshell sample
304   from the Liguangqiao Basin (Fig. 3E), a probable P-rich zone, instead of an abrupt peak, is
305   shown near the boundary between the eggshell and surrounding sediment. RS analysis indeed
306   revealed the existence of phosphates. Since RS scans a larger area than EPMA does, we suggest
307   that the absence of an abrupt peak for a P-rich zone in those 28 line-scans is a result of
308   incomplete preservation of the cuticle layer or a sampling bias during the EPMA analyses. The
309   elemental analysis also shows that P is rare in the surrounding sediment from both the Nanxiong
310   Group of China and the Two Medicine Formation of Montana, United States. The deficiency of
311   P in the sediment thus argues against an allochthonous origin of the P in the outermost part of the
312   eggshell (Figs. 3D-F & 4E). The chemometric comparison of the spectra derived from sediments
313   also suggests the depletion of phosphate minerals in the sediments. Therefore, the peak in the
314   sediment surrounding the *Triprismatoolithus stephensi* eggshell might be derived from the
315   eggshell specimen itself.
316   The enigmatic fiber-like structure near the base of the mammillary layer in the
317   *Triprismatoolithus* eggshell (Fig. 4D) may be a capillary vessel of the chorioallantoic membrane
318   or a fiber of the *membrana testacea*. The elemental analyses cannot provide evidence for the

319   preservation of the capillary vessels of the chorioallantoic membrane. SEM images show that the
320   vessels in the chorioallantoic membrane of modern chicken eggshells range in size from 3 to 10
321   μm (Maiber et al., 2016), similar to the fiber-like structure we observed in the *Triprismatoolithus*
322   eggshell (Fig. 4D). However, the fiber-like structure in the *Triprismatoolithus* eggshell does not
323   appear to be hollow, unlike a blood vessel (Schweitzer et al., 2005). It is therefore possible that
324   the enigmatic fiber-like structure in the *Triprismatoolithus* eggshell represents a part of fossilized
325   *membrana testacea*, which has never been described in theropod dinosaurs. The *membrana*
326   *testacea* fibers in a chicken egg occasionally penetrate through the mammillary base (Ahmed,
327   Suso & Hincke, 2017) and are of the same size of around 3 μm as the fiber-like structure we
328   observed in the *Triprismatoolithus* egg (Fig. 4D). However, the hypothesis of fossilized
329   *membrana testacea* requires more supporting evidence.
330
331   *Variation of P concentration in eggshells*
332   Despite numerous studies on element distribution in modern avian and reptilian eggshells,
333   dinosaur eggshells were rarely investigated from a chemical perspective. Several studies posited
334   that P is a critical element that regulates eggshell growth (Fink et al., 1993; Dennis et al., 1996;
335   Fraser, Bain & Solomon, 1999; Cusack, Fraser & Stachel, 2003). In *Gallus gallus domesticus*
336   eggshells, a pattern of increasing P concentration from the mammillary layer to the prismatic
337   layer has been reported (Cusack, Fraser & Stachel, 2003). This pattern is similar to what we
338   observed in oviraptorid eggshells (Figs. 3D-F). The deficiency of P in the surrounding sediments
339   demonstrates that the distribution pattern of P in the studied eggshells is endogenous. Since
340   ornithological research had suggested that P is an inhibitor of calcite growth during eggshell
341   formation (Fink et al., 1993; Dennis et al., 1996; Fraser, Bain & Solomon, 1999; Cusack, Fraser
342   & Stachel, 2003), the similarity of P distribution between oviraptorid dinosaur and modern avian
343   eggshells suggests that the oviraptorid dinosaurs studied by us already possessed a similar
344   eggshell formation mechanism to that of extant birds.
345   Moreover, Cusack, Fraser & Stachel (2003) also observed that the P concentration
346   increases more sharply between the mammillary and prismatic layers in the eggshell of
347   younger birds than in those of older birds. Therefore, the difference in P distribution
348   between young and older birds can probably help paleontologists decipher whether an
349   oviraptorid clutch was laid by a single female or by several females. If the whole clutch
350   was produced by a single female or by several females of a similar age, all eggs should
351   exhibit a similar pattern of P concentration increase from the mammillary layer to the
352   prismatic layer. Conversely, different patterns of increase would suggest that females of
353   different ages contributed to a single clutch. Varricchio et al. (2008) compared the ratio
354   of clutch mass to adult mass and proposed that an oviraptorid clutch was produced by
355   several females. Yang et al. (2016) have provided preliminary supportive results based on
356   statistical analyses of eggshell P distribution and external morphology in the same
357   oviraptorid clutch.
358   On the other hand, in the *Triprismatoolithus stephensi* eggshell, P concentration
359   varies slightly between the mammillary and prismatic layer but decreases significantly
360   from the prismatic layer to the external layer (Fig. 4E). Such a pattern of P distribution
361   differs from the one in oviraptorid or modern bird eggshells we discussed previously.
362   Moreover, unlike a single peak of high P concentration in oviraptorid and modern
363   eggshells, three distinctive peaks of high P concentration are present in the
364   *Triprismatoolithus stephensi* eggshell. Based on the general deficiency of P in the

365 surrounding sediment, we posit that the P peak in the sediment surrounding the
366 *Triprismatoolithus stephensi* eggshell is a result of a detached cuticle layer. The peak at
367 the boundary between the external layer and surrounding sediment represent the putative
368 cuticle layer (Fig. 4E). However, the peak at the boundary between the prismatic and
369 external layers was not reported previously in any avian eggshells (Fig. 4E). If the
370 sequestration of P is a crucial factor in the termination of calcite growth, the high
371 concentration of P on the boundary between the prismatic and external layers represents a
372 possible temporal hiatus between the prismatic and external layers in the
373 *Triprismatoolithus* eggshell.
374
375   *Interpretation of Raman spectra*
376   In the Raman study of the fossil eggshells, the peak at 967 cm^{-1} of *Gallus* eggshell was not
377 seen in all spectra, but a broad peak ranging from 972-986 cm^{-1} was detected instead (Fig. 2A).
378 The broad peak ranging from 972-986 cm^{-1} represent the phosphate groups, as indicated in Igic
379 et al. (2015) (see also Supplemental Information). Three hypotheses can be formulated to explain
380 the different spectral patterns from 960 cm^{-1} to 980 cm^{-1} in extant cuticle vs. the fossil eggshells.
381   First, theropod dinosaurs might have used whitlockite, a phosphate mineral containing
382 hydrogen phosphate anions (HPO_4^{2-}), to form the inner cuticle layer instead of HAp. Whitlockite
383 is the second most abundant mineral in biological calcified tissues, accounting for around 20% of
384 bone mineral (Driessens & Verbeeck, 1990; Jang et al., 2014; Jang et al., 2015). It is also
385 possible that the HAp of the inner cuticle layer is in a non-stoichiometric form, and hence part of
386 the phosphate anion (PO_4^{3-}) is occupied by hydrogen phosphate (HPO_4^{2-}) (Rey et al., 2011; De La
387 Pierre et al., 2014).
388   Second, the original HAp of the inner cuticle layer could have been transformed to
389 whitlockite. Jang et al. (2014) showed that HAp transforms into dicalcium phosphate dihydrate
390 (DCPD, $CaHPO_4 \cdot 2H_2O$) at 70 ℃. The DCPD is then converted into whitlockite
391 ($Ca_9(MgFe)(PO_4)_6PO_3OH$) by incorporating Mg^{2+} or Fe^{2+} when the pH decreases. In natural
392 environments, such as the Nanxiong Formation and Two Medicine Formation, burial and
393 diagenetic temperatures over 70 ℃ are unlikely except by an intrusion of igneous origin.
394 However, geological investigations did not provide any evidence for such igneous intrusions in
395 the Nanxiong Basin (Erben, 1995). At the Sevenmile Hill outcrops in Montana, United States,
396 Foreman et al. (2008) reported an altered volcanic ash layer (bentonite) that is depleted in P.
397 However, the volcanic ash layer was deposited prior to the eggshells (Jackson & Varricchio,
398 2010).
399   Third, the P we detected might be derived from the surrounding sediments during
400 diagenesis. This is inconsistent with the preservation of pigments in the Nanxiong Basin
401 eggshells and absence of igneous intrusions in both localities which suggests that the eggshells
402 we studied experienced very little diagenesis (Erben, 1995; Foreman et al., 2008; Wiemann et
403 al., 2017).
404
405   *Pigmentation on theropod eggshells*
406   As noted above, the discovery of protoporphyrin (Wiemann et al., 2017) in oviraptorid
407 dinosaur eggshells from all three localities where the eggshells for this study were collected
408 (Table 1) is consistent with the cuticle preservation. Although Wilson et al. (2017) indicated that
409 pigment deposition and cuticle formation are not codependent, the preserved protoporphyrin
410 pigments was probably from the cuticle layer.

411   Thomas et al. (2015) performed Raman spectroscopy and mass spectrometry to show the
412   detectability of pigments in extant avian eggshells. Our Raman analyses also demonstrate
413   detectability of pigments in fossil eggshells; however, the peaks in the spectra do not completely
414   correspondent with the ones shown in Thomas et al. (2015), suggesting further Raman studies
415   using mass spectrometry on dinosaur eggshells.
416
417   *Nesting ecology of oviraptorid dinosaurs*
418   As noted, two nesting modes are recognized in birds, open and buried nesting (Varricchio &
419   Jackson, 2016). Most birds build open nests either on the tree or on the ground (ostriches or
420   emus), while the megapode birds bury their eggs in a mound. Therefore, all open-nesting birds
421   have eggshells of low porosity (Tanaka, Zelenitsky & Therrien, 2015). However, an intermediate
422   mode, semi-open nests in oviraptorid dinosaurs, was recently proposed based on detection of
423   pigments and porosity evaluation (Yang et al., 2015; Wiemann et al., 2017). Pigmented eggshells
424   strongly suggest an open nesting mode. However, the porosity evaluation revealed a
425   heterogeneous distribution of porosity—highest porosity in the lower middle part (buried) and
426   lowest porosity in the blunt end (open) (Yang et al., 2015; Wiemann et al., 2017), thus indicating
427   a semi-open nesting mode. This intermediate mode is consistent with the fluvial environment
428   inferred by sedimentological investigations in the Nanxiong Basin (Erben, 1995). In such a
429   humid fluvial environment, the risk of microbial invasions was much higher. The cuticular
430   nanospheres, which are associated with humid environments and protect extant eggs from
431   microbial invasions, were likely present in the oviraptorid and alvarezsaurid dinosaur eggs from
432   these fossil humid environments as well. Although we did not detect cuticular nanospheres in the
433   dinosaur eggshell, our detection of a cuticle layer suggests it to have been an adaptation the
434   oviraptorid and alvarezsaurid dinosaurs nesting in a humid fluvial environment (D'Alba et al.,
435   2016).
436   On the other hand, it was inferred that Mongolian oviraptorid clutches were deposited in a
437   xeric environment. The evidence is the eolian nature (sand dune deposits) in the Baruungoyot
438   and the Djadokhta formations (Norell et al., 1995). Although no Mongolian oviraptorid eggshells
439   were included in our study, it appears likely that Mongolian oviraptorid eggs were also cuticle-
440   coated for the prevention of water loss as in Adélie penguin eggs (Thompson & Goldie, 1990).
441   Fanti, Currie & Demchig (2012) documented clutches of the oviraptorid *Nemegtomaia* from both
442   the Nemegt and Baruungoyot formations, that represent mesic and xeric habitats, respectively.
443   Moreover, they also provided evidence for the lateral coexistence of mesic and xeric habitats in
444   the Baruungoyot Formation and posited that *Nemegtomaia* and other Mongolian oviraptorid
445   dinosaurs nested near permanent or seasonal streams. In such a variable environment, the cuticle-
446   coated eggs, therefore, would have been an adaptive trait that enhanced reproductive success of
447   oviraptorid dinosaurs.
448   While it is uncertain that the alvarezsaurid eggshells were pigmented without further
449   chemical studies, it is possible that alvarezsaurid dinosaur exploited similar nesting strategies as
450   oviraptorid dinosaurs did.
451
452   *Taphonomic implications for cuticle preservation*
453   The cuticle layer is a labile, easily lost structure that appears unlikely to be preserved during
454   the fossilization process. Our study thus raises an important taphonomic question, i.e., how did
455   the cuticle layer get preserved? Since the cuticle preservation observed by us appears to pertain
456   to eggshell from clutches and not from dispersed eggshell, cuticle preservation probably is

457 facilitated by fossilization of eggs in clutches. Furthermore, a layer of secondary diagenetic
458 calcite is commonly observed on eggshells from fluvial deposits (Fig. 3A; Jackson et al., 2010).
459 This layer of secondary calcite may have been a rigid shield that protected the cuticle layer from
460 mechanical removal.
461   Therefore, we hypothesize that the *in situ* preservation and the coverage of secondary
462 calcite possibly protect the cuticle layer from being washed away or removed. More detailed
463 microscopic observation of the association between the cuticle, secondary calcite layers, and
464 surrounding sediment will possibly elucidate the taphonomic processes.
465
466 **Conclusions**
467   Our study suggests preservation of the inner cuticle layer in *Macroolithus yaotunensis* and
468 *Triprismatoolithus stephensi* eggs based on elemental analysis and RS. The cuticle layer and a
469 semi-open nesting mode in humid environments may be key adaptations to protect the eggs from
470 microbial invasions in a humid environment such as a fluvial plain, as does the cuticle layer of
471 extant birds nesting in humid environments. In combination with the previous discovery of
472 pigments in oviraptorid dinosaur eggshells, this study provides further evidence for preservation
473 of soft tissues in the fluvial deposits, especially in the Cretaceous red bed basins of China.
474 Further chemical studies on dinosaur eggshells will shed additional light on the reproductive
475 biology of dinosaurs, as well as on taphonomic questions.
476
477 **Institutional and technical abbreviations**
478 **EPMA**   Electron probe microanalysis
479 **RS**   Raman spectroscopy
480 **MOR**   Museum of the Rockies, Bozeman, Montana, U.S.A
481 **MPIE**   Max-Planck-Institute for Iron Research, Dusseldorf, Germany
482 **NMNS**   National Museum of Natural Sciences, Taichung, Taiwan
483 **SEM**   Scanning electron microscopy
484 **STIPB**   Steinmann-Institute for Geology, Mineralogy, und Paleontology, University of Bonn,
485   Bonn, Germany
486 **TEM**   Transmission electron microscopy
487 **WDS**   Wavelength Dispersive Spectrometer
488 **ZAF**   Matrix correction factors. Z, atomic number correction; A, absorption correction; F,
489   characteristic fluorescence correction
490
491
492 **Acknowledgements**
493   The SEM observations and EPMA analyses were performed at the Steinmann-Institute of
494 the University of Bonn, Bonn, Germany. Prof. Dr. Andreas Erbe and Ms. Petra Ebbinghaus
495 kindly provided the access to the WItec Raman and Horiba Jobin Yvon Raman spectrometers at
496 the **MPIE**. Fossil eggshell samples were provided by Prof. David Varricchio at the Montana
497 State University, Dr. Georg Heumann at the STIPB, and Prof. Dr. Yen-Nien Cheng at the
498 NMNS. This is contribution number 1 of DFG Research Unit 2685 "The Limits of the Fossil
499 Record: Analytical and Experimental Approaches to Fossilization. "

References

Agnolin FL, Powell JE, Novas FE, Kundrát M. 2012. New alvarezsaurid (Dinosauria, Theropoda) from uppermost Cretaceous of north-western Patagonia with associated eggs. *Cretaceous Research* 35:33-56. DOI: 10.1016/j.cretres.2011.11.014

Ahmed TAE, Suso H-P, Hincke MT. 2017. In-depth comparative analysis of the chicken eggshell membrane proteome. *Journal of Proteomics* 155:49-62. DOI: 10.1016/j.jprot.2017.01.002

Board RG. 1982. Properties of avian egg shells and their adaptive value. *Biological Reviews* 57:1-28. DOI:10.1111/j.1469-185X.1982.tb00362.x

Board RG, Fuller R. 1974. Non-specific antimicrobial defences of the avian egg, embryo, and neonate. *Biological Reviews* 49:15-49. DOI: 10.1111/j.1469-185X.1974.tb01297.x

Board RG, Halls NA. 1973. The cuticle: A barrier to liquid and particle penetration of the shell of the hen's egg. *British Poultry Science* 14:69-97. DOI: 10.1080/00071667308415999

Chen L, Steel, RJ, Guo F, Olariu C, Gong C. 2017. Alluvial fan facies of the Yongchong Basin: Implications for tectonic and paleoclimatic changes during Late Cretaceous in SE China. *Journal of Asian Earth Sciences* 134:37-54. DOI: 10.1016/j.jseaes.2016.10.010

Cheng Y-N, Ji C, Wu X, Shan H-Y. 2008. Oviraptorosaurian eggs (Dinosauria) with embryonic skeletons discovered for the first time in China. *Acta Geologica Sinica* 82:1089-1094. DOI: 10.1111/j.1755-6724.2008.tb00708.x

Chow M. 1954. Additional notes on the microstructure of the supposed dinosaurian eggshells from Laiyang, Shantung. *Acta Palaeontologica Sinica* 2:389-394.

Crane NJ, Popescu V, Morris MD, Steenhuis P, Ignelzi MA. 2006. Raman spectroscopic evidence for octacalcium phosphate and other transient mineral species deposited during intramembranous mineralization. *Bone* 39:434-442. DOI: 10.1016/j.bone.2006.02.059

Cusack M, Fraser AC, Stachel T. 2003. Magnesium and phosphorus distribution in the avian eggshell. *Comparative Biochemistry and Physiology Part B: Biochemistry and Molecular Biology* 134:63-69. DOI: 10.1016/S1096-4959(02)00185-9

D'Alba L, Jones DN, Badawy HT, Eliason CM, Shawkey, MD. 2014. Antimicrobial effects of a nanostructured eggshell in a compost-nesting bird. *Journal of Experimental Biology* 217: 1116–1121. DOI: 10.1111/ibi.12527

D'Alba L, Maia R, Hauber ME, Shawkey MD. 2016. The evolution of eggshell cuticle in relation to nesting ecology. *Proceedings of the Royal Society B: Biological Sciences* 283. DOI: 10.1098/rspb.2016.0687

D'Alba L, Torres R, Waterhouse GIN, Eliason C, Hauber ME, Shawkey MD. 2017. What does the eggshell cuticle do? A functional comparison of avian eggshell cuticles. *Physiological and Biochemical Zoology* 90:588-599. DOI:10.1086/693434

De La Pierre M, Carteret C, Maschio L, André E, Orlando R, Dovesi R. 2014. The Raman spectrum of $CaCO_3$ polymorphs calcite and aragonite: a combined experimental and computational study. *The Journal of chemical physics* 140:164509. DOI: 10.1063/1.4871900

Deeming DC. 1987. Effect of cuticle removal on the water vapour conductance of egg shells of several species of domestic bird. *British Poultry Science* 28:231-237. DOI: 10.1080/00071668708416957

Deeming DC. 2006. Ultrastructural and functional morphology of eggshells supports the idea that dinosaur eggs were incubated buried in a substrate. *Palaeontology* 49:171-185. DOI: 10.1111/j.1475-4983.2005.00536.x

546 Dennis JE, Xiao SQ, Agarwal M, Fink DJ, Heuer AH, Caplan AI. 1996. Microstructure of matrix
547 and mineral components of eggshells from White Leghorn chickens (*Gallus gallus*).
548 *Journal of Morphology* 228:287-306.
549 Driessens FCM, Verbeeck RK. 1990. *Biominerals*. Boca Raton, FL: CRC Press.
550 Erben HK. 1995 (ed.). *Die Kreide/Tertiär-Grenze im Nanxiong-Becken: Kontinentalfazies,*
551 *Südostchina*. Stuttgart: Franz Steiner Verlag GmbH.
552 Fanti F, Currie PJ, Demchig B. 2012. New Specimens of *Nemegtomaia* from the Baruungoyot
553 and Nemegt Formations (Late Cretaceous) of Mongolia. *PLoS One* 7: e31330. DOI:
554 10.1371/journal.pone.0031330
555 Fecheyr-Lippens DC, Igic B, D'Alba L, Hanley D, Verdes A, Holford M, Waterhouse GIN,
556 Grim T, Hauber ME, Shawkey MD. 2015. The cuticle modulates ultraviolet reflectance
557 of avian eggshells. *Biology Open* 4:753-759. DOI: 10.1242/bio.012211
558 Ferguson MWJ. 1982. The structure and composition of the eggshell and embryonic membranes
559 of Alligator mississippiensis. *The Transactions of the Zoological Society of London*
560 36:99-152. DOI: 10.1111/j.1096-3642.1982.tb00064.x
561 Fink DJ, Kuhn LT, Caplan AI, Huer AH. 1993. Eggshell assembly, a model for biomimetic
562 ceramic production. In: Nys Y, ed. Fifth European Symposium on the Quality of Egg and
563 Egg Products. Tours: WPSA. p. A1-A6.
564 Foreman BZ, Rogers RR, Deino AL, Wirth KR, Thole JT. 2008. Geochemical characterization
565 of bentonite beds in the Two Medicine Formation (Campanian, Montana), including a
566 new $^{40}Ar/^{39}Ar$ age. *Cretaceous Research* 29:373-385. DOI: 10.1016/j.cretres.2007.07.001
567 Fraser AC, Bain MM, Solomon SE. 1999. Transmission electron microscopy of the vertical
568 crystal layer and cuticle of the eggshell of the domestic fowl. *British Poultry Science*
569 40:626-631. DOI: 10.1080/00071669987016
570 Frost RL, Scholz R, López A, Xi Y. 2014. A vibrational spectroscopic study of the phosphate
571 mineral whiteite $CaMn^{++}Mg_2Al_2(PO_4)_4(OH)_2\cdot8(H_2O)$. *Spectrochimica Acta Part A:*
572 *Molecular and Biomolecular Spectroscopy* 124:243-248. DOI: 10.1016/j.saa.2014.01.053
573 Gergely G, Wéber F, Lukács I, Tóth AL, Horváth ZE, Mihály J, Balázsi C. 2010. Preparation
574 and characterization of hydroxyapatite from eggshell. *Ceramics International* 36:803-
575 806. DOI: 10.1016/j.ceramint.2009.09.020
576 Grellet-Tinner G. 2005. *Membrana testacea* of titanosaurid dinosaur eggs from Auca Mahuevo
577 (Argentina): Implications for exceptional preservation of soft tissue in Lagerstätten.
578 *Journal of Vertebrate Paleontology* 25:99-106. DOI: 10.1671/0272-
579 4634(2005)025[0099:mtotde]2.0.co;2
580 Grellet-Tinner G, Fiorelli LE. 2010. A new Argentinean nesting site showing neosauropod
581 dinosaur reproduction in a Cretaceous hydrothermal environment. *Nature*
582 *Communications* 1:32. DOI: 10.1038/ncomms1031
583 Hanson BA. 2017. ChemoSpec: Exploratory Chemometrics for Spectroscopy, *R package version*
584 4.4.97.
585 He F, Huang X, Li X. 2017. Occurrence rule and buried characteristics of dinosaur fossils in the
586 Ganzhou Basin, Jiangxi Province. *East China Geology* 38:250-254.
587 DOI:10.16788/j.hddz.32-1865/P.2017.04.002
588 Hechenleitner EM, Grellet-Tinner G, and Fiorelli LE. 2015. What do giant titanosaur dinosaurs
589 and modern Australasian megapodes have in common? *PeerJ* 3:e1341. DOI:
590 10.7717/peerj.1341
591 Igic B, Fecheyr-Lippens D, Xiao M, Chan A, Hanley D, Brennan PRL, Grim T, Waterhouse

On

592   GIN, Hauber ME, Shawkey MD. 2015. A nanostructural basis for gloss of avian
593   eggshells. *Journal of The Royal Society Interface* 12:20141210. DOI:
594   10.1098/rsif.2014.1210

595 Jackson FD. 2007. Titanosaur reproductive biology: comparison of the Auca Mahuevo titanosaur
596   nesting locality (Argentina), to the Pinyes *Megaloolithus* nesting locality (Spain). Ph.D.
597   Thesis, Montana State University.

598 Jackson FD, Varricchio DJ. 2010. Fossil eggs and eggshell from the lowermost Two Medicine
599   Formation of western Montana, Sevenmile Hill locality. *Journal of Vertebrate*
600   *Paleontology* 30:1142-1156. DOI: 10.1080/02724634.2010.483537

601 Jang HL, Jin K, Lee J, Kim Y, Nahm SH, Hong KS, Nam KT. 2014. Revisiting whitlockite, the
602   second most abundant biomineral in bone: nanocrystal synthesis in physiologically
603   relevant conditions and biocompatibility evaluation. *ACS Nano* 8:634-641. DOI:
604   10.1021/nn405246h

605 Jang HL, Lee HK, Jin K, Ahn H-Y, Lee H-E, Nam KT. 2015. Phase transformation from
606   hydroxyapatite to the secondary bone mineral, whitlockite. *Journal of Materials*
607   *Chemistry B* 3:1342-1349. DOI: 10.1039/c4tb01793e

608 Kennedy GY, Vevers HG. 1976. A survey of avian eggshell pigments. *Comparative*
609   *Biochemistry and Physiology Part B: Comparative Biochemistry* 55:117-123. DOI:
610   10.1016/0305-0491(76)90183-8

611 Kohring R, Hirsch KF. 1996. Crocodilian and avian eggshells from the Middle Eocene of the
612   Geiseltal, Eastern Germany. *Journal of Vertebrate Paleontology* 16:67-80. DOI:
613   10.1080/02724634.1996.10011285

614 Kusada S, Iwasawa A, Doi O, Ohya Y, Yoshizaki N. 2011. Diversity of the cuticle layer of avian
615   eggshells. *Journal of Poultry Science* 48:119-124. DOI: 10.2141/jpsa.010103.

616 Maiber M, Reglin B, Nitzsche B, Xiang W, Rong WW, Hoffmann B, Djonov V, Secomb TW,
617   Pries AR. 2016. Structure and hemodynamics of vascular networks in the chorioallantoic
618   membrane of the chicken. *American Journal of Physiology* 311:913-926. DOI:
619   10.1152/ajpheart.00786.2015

620 Mikhailov KE. 1991. Classification of fossil eggshells of amniotic vertebrates. *Acta*
621   *Palaeontologica Polonica* 36.

622 Mikhailov KE, Ornithologists' Club B. 1997. *Avian Eggshells: An Atlas of Scanning Electron*
623   *Micrographs*. Tring: British Ornithologists' Club.

624 Mikšík I, Eckhardt A, Sedláková P, Mikulikova K. 2007. Proteins of insoluble matrix of avian
625   (*Gallus gallus*) eggshell. *Connective Tissue Research* 48:1-8. DOI:
626   10.1080/03008200601003116

627 Norell MA, Clark JM, Chiappe LM, Dashzeveg D. 1995. A nesting dinosaur. *Nature* 378:774-
628   776. DOI: 10.1038/378774a0

629 Nys Y, and Guyot N. 2011. Egg formation and chemistry. In: Nys Y, Bain M, and van
630   Immerseel F, eds. *Improving the Safety and Quality of Eggs and Egg Products*.
631   Cambridge: Woodhead Publishing, p. 83-132.

632 Nys Y, Zawadzki J, Gautron J, Mills A. 1991. Whitening of brown-shelled eggs: mineral
633   composition of uterine fluid and rate of protoporphyrin deposition. *Poultry Science*
634   70:1236-1245.

635 Oskam CL, Haile J, McLay E, Rigby P, Allentoft ME, Olsen ME, Bengtsson C, Miller GH,
636   Schwenninger J-L, Jacomb C, Walter R, Baynes A, Dortch J, Parker-Pearson M, Gilbert
637   MTP, Holdaway RN, Willerslev E, Bunce M. 2010. Fossil avian eggshell preserves

638   ancient DNA. *Proceedings of the Royal Society of London B: Biological Sciences*
639   277:1991-2000. DOI: 10.1098/rspb.2009.2019

640   Packard MJ, DeMarco VG. 1991. Eggshell structure and formation in eggs of oviparous reptiles.
641   In: Deeming, CD, Ferguson MWJ, eds. *Egg Incubation: Its Effects on Embryonic*
642   *Development in Birds and Reptiles*. Cambridge: Cambridge University Press.

643   Rahman MA, Moriyama A, Iwasawa A, Yoshizaki N. 2009. Cuticle formation in quail eggs.
644   *Zoological Science* 26:496-499. DOI: 10.2108/zsj.26.496

645   Reisz RR, Huang TD, Roberts EM, Peng S, Sullivan C, Stein K, LeBlanc ARH, Shieh D, Chang
646   R, Chiang C, Yang C, Zhong S. 2013. Embryology of Early Jurassic dinosaur from China
647   with evidence of preserved organic remains. *Nature* 496:210-214. DOI:
648   10.1038/nature11978

649   Rey C, Combes C, Drouet C, Grossin D. 2011. Bioactive ceramics: Physical chemistry. In:
650   Ducheyne P, Healy K, Hutmacher D, Grainger DE, Kirkpatrick J, eds. *Comprehensive*
651   *Biomaterials*. Oxford: Elsevier, p. 187-221.

652   Rodríguez-Navarro AB, Domínguez-Gasca N, Muñoz A, Ortega-Huertas M. 2013. Change in the
653   chicken eggshell cuticle with hen age and egg freshness. *Poultry Science* 92:3026-3035.
654   DOI: 10.3382/ps.2013-03230

655   Romanoff AL, Romanoff AJ. 1949. *The Avian Egg*. Hoboken, NJ: John Wiley & Sons Inc.

656   Sander PM, Peitz C, Gallemi J, Cousin R. 1998. Dinosaur nesting on a red beach? *Comptes*
657   *Rendus de l'Académie des Sciences* 327:67-74.

658   Sander PM, Peitz C, Jackson FD, Chiappe LM. 2008. Upper Cretaceous titanosaur nesting sites
659   and their implications for sauropod dinosaur reproductive biology. *Palaeontographica*
660   *Abteilung A*:69-107.

661   Sauer GR, Zunic WB, Durig JR, Wuthier RE. 1994. Fourier transform Raman spectroscopy of
662   synthetic and biological calcium phosphates. *Calcified Tissue International* 54:414-420.
663   DOI: 10.1007/bf00305529

664   Schwartz S, Stephenson BD, Sarkar DH, Bracho MR. 1975. Red, white, and blue eggs as models
665   of porphyrin and heme metabolism. *Annals of the New York Academy of Sciences*
666   244:570-588.

667   Schweitzer MH, Wittmeyer JL, Horner JR, Toporski JK. 2005. Soft-tissue vessels and cellular
668   preservation in *Tyrannosaurus rex*. *Science* 307:1952-1955.
669   DOI:10.1126/science.1108397

670   Simons PCM. 1971. Ultrastructure of hen's egg physiological interpretation. Ph.D. Dissertation,
671   Agricultural University.

672   Sochava AV. 1971. Two types of egg shells of Senonian dinosaurs. *Paleontologicheskii Zhurnal*
673   3:80-88.

674   Tanaka K, Zelenitsky DK, Therrien F. 2015. Eggshell porosity provides insight on evolution of
675   nesting in dinosaurs. *PLoS ONE* 10:e0142829. DOI: 10.1371/journal.pone.0142829

676   Thomas DB, Hauber ME, Hanley D, Waterhouse GIN, Fraser S, Gordon KC. 2015. Analysing
677   avian eggshell pigments with Raman spectroscopy. *The Journal of Experimental Biology*
678   218:2670-2674. DOI: 10.1242/jeb.124917

679   Thompson MB, Goldie KN. 1990. Conductance and structure of eggs of Adelie penguins,
680   *Pygoscelis adeliae*, and its implications for incubation. *The Condor* 92:304-312.
681   DOI:10.2307/1368228

682   Varricchio DJ, Jackson F, Borkowski JJ, Horner JR. 1997. Nest and egg clutches of the dinosaur
683   *Troodon formosus* and the evolution of avian reproductive traits. *Nature* 385:247-250.

684 Varricchio DJ, Jackson FD. 2004. A phylogenetic assessment of prismatic dinosaur eggs from
685  the Cretaceous Two Medicine Formation of Montana. *Journal of Vertebrate*
686  *Paleontology* 24:931-937. DOI: 10.1671/0272-4634(2004)024[0931:apaopd]2.0.co;2
687 Varricchio DJ, Jackson FD. 2016. Reproduction in Mesozoic birds and evolution of the modern
688  avian reproductive mode. *The Auk* 133:654-684. DOI: 10.1642/auk-15-216.1
689 Varricchio DJ, Jackson FD, Jackson RA, Zelenitsky DK. 2013. Porosity and water vapor
690  conductance of two *Troodon formosus* eggs: an assessment of incubation strategy in a
691  maniraptoran dinosaur. *Paleobiology* 39:278-296. DOI: 10.1666/11042
692 Varricchio DJ, Moore JR, Erickson GM, Norell MA, Jackson FD, Borkowski JJ. 2008. Avian
693  paternal care had dinosaur origin. *Science* 322:1826-1828. DOI:
694  10.1126/science.1163245
695 Vila B, Jackson FD, Fortuny J, Sellés AG, Galobart À. 2010. 3-D modelling of megaloolithid
696  clutches: Insights about nest construction and dinosaur behaviour. *PLoS ONE* 5:e10362.
697  DOI: 10.1371/journal.pone.0010362
698 Walters MA, Leung YC, Blumenthal NC, Konsker KA, LeGeros RZ. 1990. A Raman and
699  infrared spectroscopic investigation of biological hydroxyapatite. *Journal of Inorganic*
700  *Biochemistry* 39:193-200. DOI: 10.1016/0162-0134(90)84002-7
701 Wedral EM, Vadehra DV, Baker RC. 1974. Chemical composition of the cuticle, and the inner
702  and outer shell membranes from eggs of *Gallus gallus*. *Comparative Biochemistry and*
703  *Physiology Part B: Comparative Biochemistry* 47:631-640. DOI: 10.1016/0305-
704  0491(74)90011-X
705 Wiemann J, Yang T-R, Sander PN, Schneider M, Engeser M, Kath-Schorr S, Müller CE, Sander
706  PM. 2017. Dinosaur origin of egg color: oviraptors laid blue-green eggs. *PeerJ* 5:e1323.
707  DOI: 10.7717/peerj.3706
708 Wilson PW, Suther CS, Bain MM, Icken W, Jones A, Quinlan-Pluck F, Olori V, Gautron J,
709  Dunn IC. 2017. Understanding avian egg cuticle formation in the oviduct: a study of its
710  origin and deposition. *Biology of Reproduction* 97:39-49. DOI:10.1093/biolre/iox070
711 Yang T-R, Sander PM, Wiemann J, Cheng Y-N. 2015. Reproductive biology of the oviraptorid
712  dinosaurs revealed by the interpreted egg inner structures. In: Canoville P, Mitchel J,
713  Stein K, Konietzko-Meier D, Teschner E, van Heteren A, Sander PM, eds. *Program and*
714  *Abstracts Book of the Third International Symposium of Paleohistology*. Bonn, Germany.
715  p. 33.
716 Yang T-R, van Heteren A, Wiemann J, Chen C-J, Spiering B. 2016. Communal nesting behavior
717  of dinosaurs revealed by statistical analyses of phosphorus distribution in, and external
718  morphology of, eggshells. In: Farke A, MacKenzie A, Miller-Camp J, eds. *Program and*
719  *Abstracts Book of the 76th SVP Annual Meeting. Salt Lake City, Utah, United States:*
720  *Society of Vertebrate Paleontology*. p. 255.
721 Zhang S. 2009. Hugang Formation. In: Zhang S, ed. *Geological Formation Names of China*
722  *(1866–2000)*. Berlin: Springer Verlag, p. 466.
723 Zhao, Z. 1975. Microstructures of the dinosaurian eggshells of Nanxiong, Guangdong, and the
724  problems in egg classification. *Vertebrata Palasiatica* 13(2):105-117.

Figure 1

Cross-sectional view, SEM images, and Raman imaging and spectrum of a *Gallus gallus domesticus* egg and eggshell.

The Raman image and spectrum were collected using 532 nm excitation wavelength and a 50x objective with RI. (A) The generalized anatomy of an egg. (B) The chicken eggshell comprises three crystalline layers, including the mammillary layer, prismatic layer, and external layer. The cuticle layer overlying the calcareous eggshell is further divided to two layers, including a HAp inner layer and a proteinaceous outer layer. The shell membrane, namely *membrane testacea*, is also characterized by two layers. (C) SEM image of the cuticle on the surface of the *Gallus* eggshell, showing a patchy and cracking pattern. (D) SEM image of the radial section of the *Gallus* eggshell. The white arrow indicates the cuticle layer that lies on the calcitic eggshell. (E) Raman chemical image with peak targeting at 967 cm^{-1} which is attributed to HAp. The yellow area represents the patchy distribution of the inner HAp cuticle layer on the *Gallus* eggshell. The calcitic eggshell that is not covered by the inner HAp cuticle layer is shown in the brown area. The dotted circle corresponds to the spectrum shown in (F). (F) Spectrum collected in the dotted-circle area of the Raman chemical image shown in (E). Two significant peaks at 967 cm^{-1} and 1087 cm^{-1} represent HAp and calcite, respectively. Credit of the SEM images and drawings: Tzu-Ruei Yang (Universität Bonn).
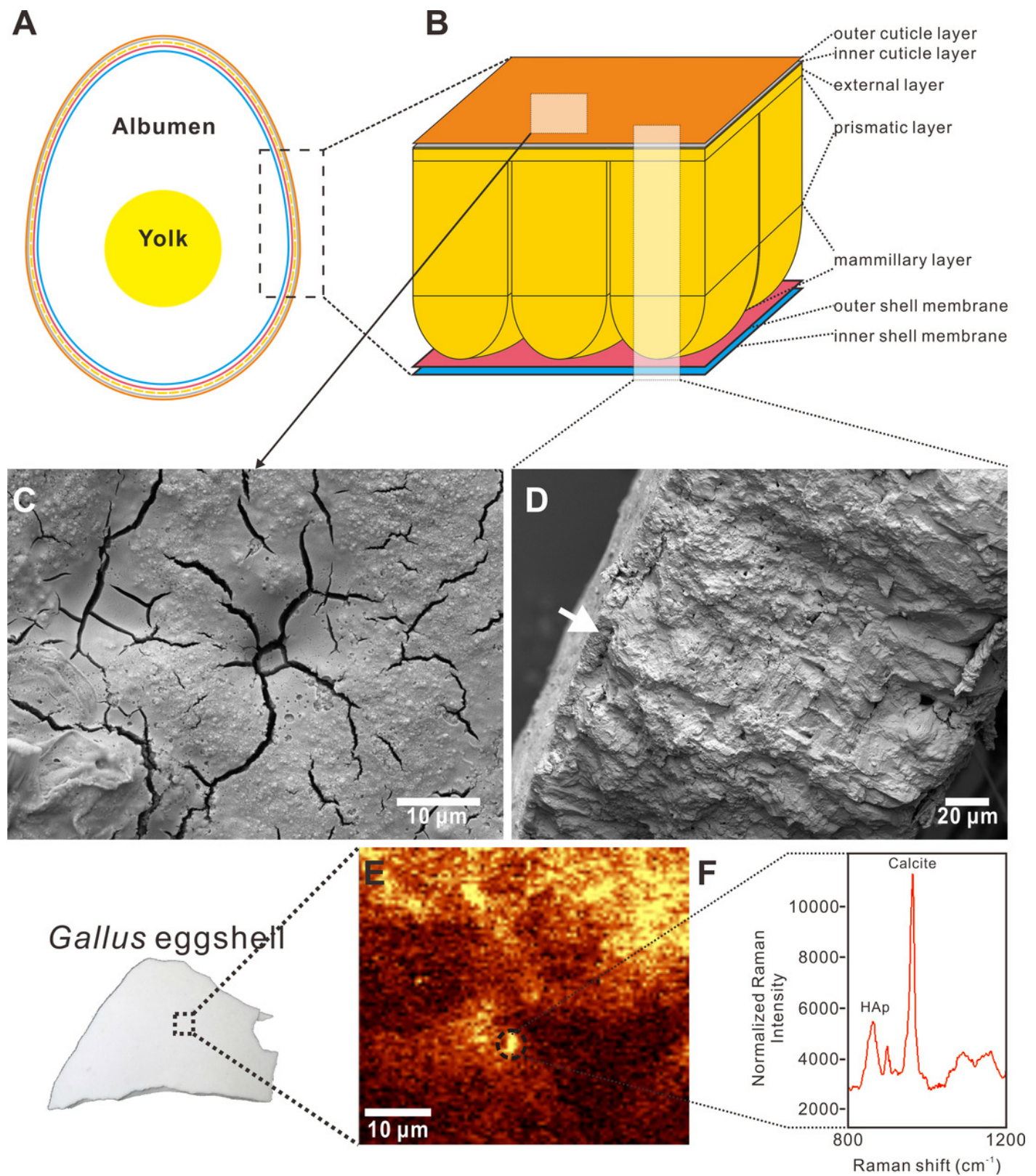
Figure 2

Raman spectra and chemometric analysis.

(A) Raman spectra derived from chicken, crocodilian, fossil dinosaur eggshells, and surrounding sediments. The peaks around 972-986 cm^{-1} and 1063-1097 cm^{-1} are marked by yellow bars, indicating the calcite and phosphate bonds. (B) The principle component chemometric analysis on the spectral area of 800-1200 cm^{-1} shown in (A) demonstrates significant disparities between dinosaur/chicken eggshells, crocodilian eggshells, and sediments. Credit of the drawings: Tzu-Ruei Yang (Universität Bonn).
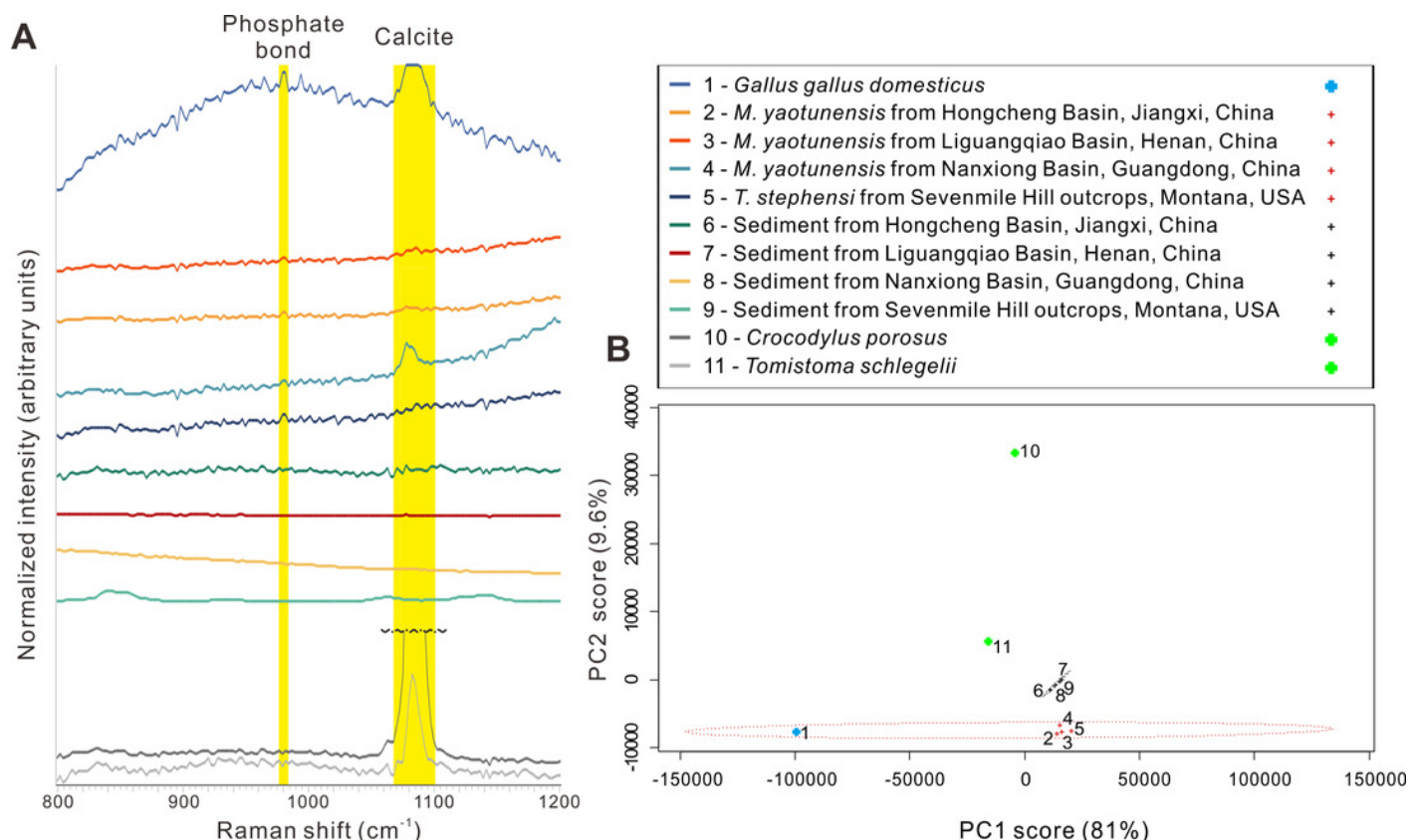
Figure 3

Microscopic images of *Macroolithus yaotunensis* eggshell from Henan, Jiangxi, and Guangdong and their line-scan spectra.

(A) The *Macroolithus yaotunensis* eggshell (NMNS CYN-2004-DINO-05-I) from Jiangxi under the polarized light microscope. The red arrows indicate the indistinct boundary between the sediment and an enigmatic layer. This enigmatic layer probably was formed by the interaction between organics of the egg and surrounding sediment. The location of the EPMA line-scan spectra in (D) is indicated by the white solid line. In this eggshell image, a smooth boundary between the prismatic and mammillary layers (PL and ML, seen as dark and light zones) is clearly observed. (B) SEM image of radial untreated fracture of the *Macroolithus yaotunensis* eggshell. The boundary between the sediment and prismatic layer is marked by yellow dashed line based on their distinct structural features. The boundary between ML and PL is marked by the red dashed line. The ML shows the distinct vertical mammillae structure. (C) Close-up image of the area in white box in (B). Possible preservation of cuticle is indicated by the white arrow, showing patchy and flaky structures similar to the cuticle on the modern chicken eggshell (Figs. 1C & 1D). (D)-(F) The microscopic image to the left of the spectra shows the radial cut section of studied *Macroolithus yaotunensis* eggshells seen in the SEM coupled with the EPMA and elemental line-scan track marked as black lines. (D) The spectra illustrate the distribution of Ca and P across the eggshell from the Hongcheng Basin in Jiangxi shown in (A), from innermost (left) to outermost, as indicated by the white line in the microscopic image. The Ca spectrum clearly marks the extent of the calcitic eggshell. A significant peak that is marked by a black arrow demonstrates a relatively high concentration of P, indicating the possible preservation of the cuticular HAp layer. (E) The spectra illustrate the distribution of Ca and P across the eggshell from the Liguangqiao Basin in Henan, from innermost (left) to outermost. The Ca spectrum clearly marks the extent of the calcitic eggshell. A slightly higher amount of P near the interface between the eggshell and

sediments, as indicated by a black arrow, is observed. (F) The spectra illustrate the distribution of Ca and P across the eggshell from the Nanxiong Basin in Guangdong, from innermost (left) to outermost. A significant peak that is marked by a black arrow demonstrates a relatively high concentration of P, indicating the possible preservation of the cuticular HAp layer. ML, mammillary layer; PL, prismatic layer. Credit of the SEM images and drawings: Tzu-Ruei Yang (Universität Bonn).
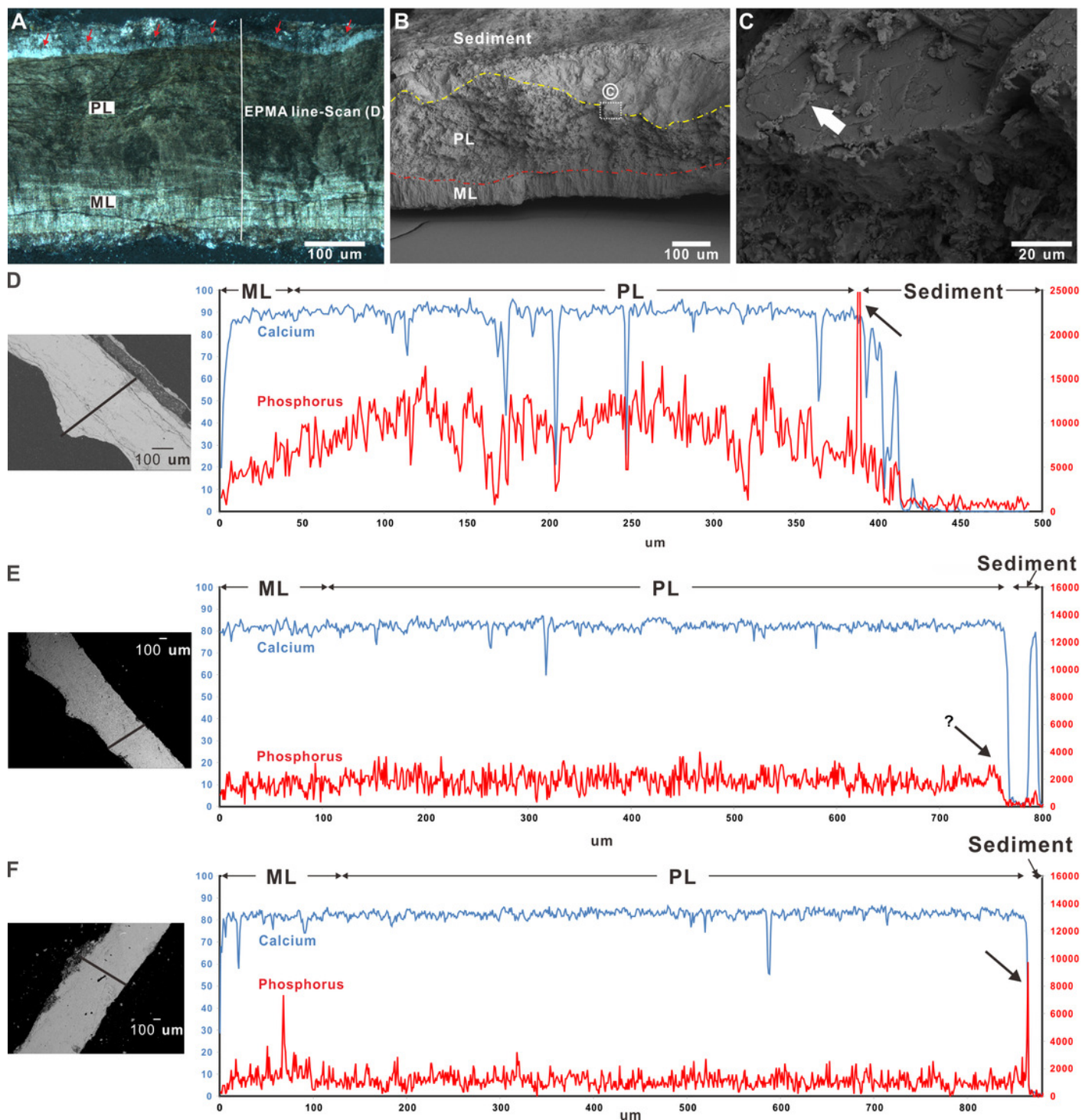
Figure 4

SEM images of the *Triprismatoolithus* eggshell and EPMA line-scan spectra.

(A) The radial cut section of studied *Triprismatoolithus* eggshell in the SEM coupled with the EPMA. (B) The probable flake-like cuticle structure atop the eggshell, marked by the white arrow. The red dotted line marks the outermost boundary of the prismatic layer. (C) An enigmatic structure (white arrow) protruding from the mammillary layer, possibly a fiber of the *membrana testacea* extending into the mammillary layer. (D) Enlargement of the possible fiber. (E) Line scans across eggshell in (A). The scan shows a high concentration of P at the boundary between the eggshell and surrounding sediment. Two other peaks of P were observed on the boundary between the external and prismatic layer and in the sediment. The P concentration does not differ between the mammillary and prismatic layers; however, the external layer showed a significantly lower concentration of P than the mammillary and prismatic layers. EL, external layer; ML, mammillary layer; PL, prismatic layer. Credit of the SEM images and drawings: Tzu-Ruei Yang (Universität Bonn).
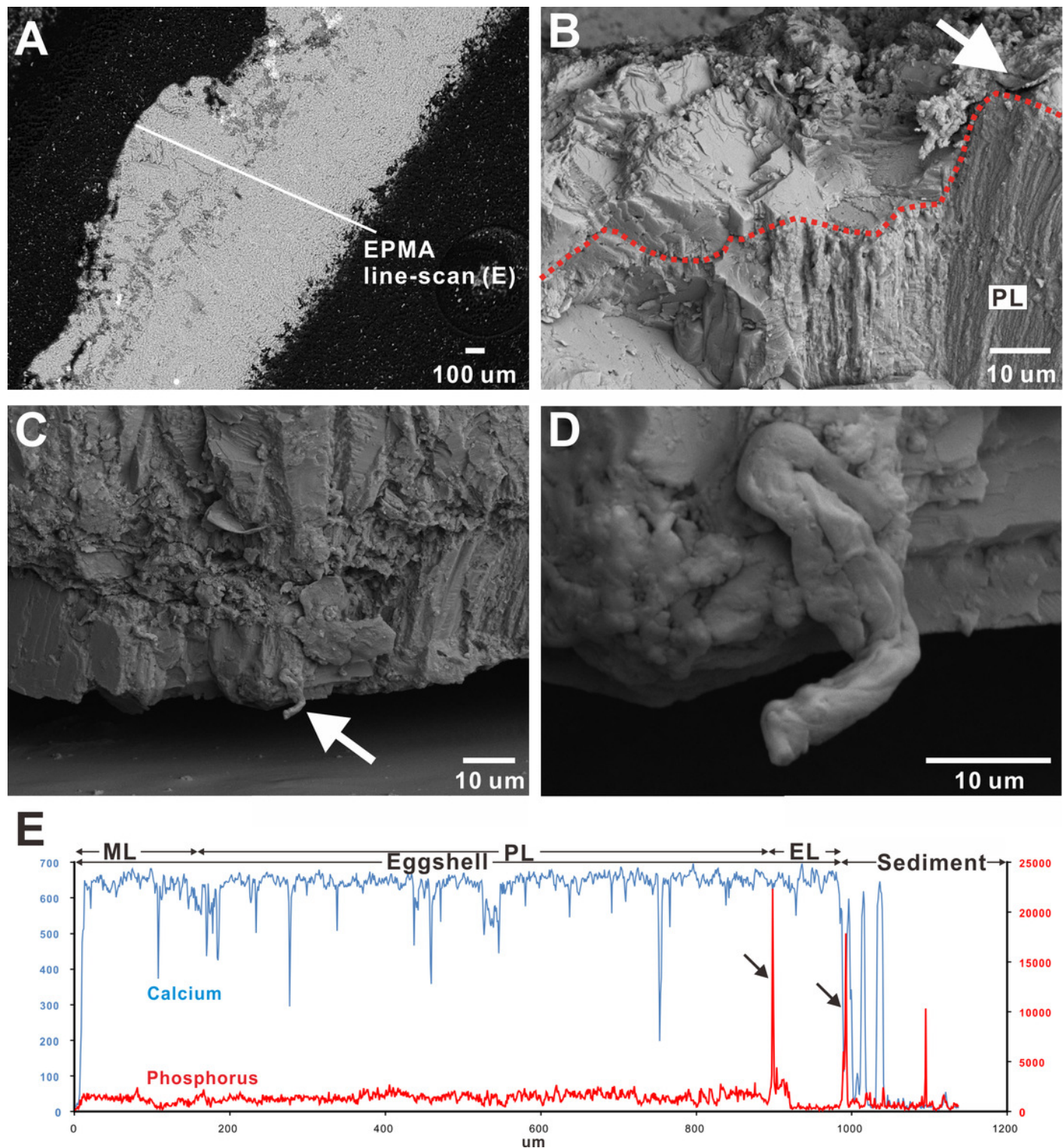
Eggshells analyzed in this study

The ootaxonomic/taxonomic assignments, stratigraphic and locality information, and catalog numbers of the eggshells analyzed in this study

1 **Tables**

2 **Table 1**   Eggshells analyzed in this study.

Oospecies or species	Stratigraphy	Locality	Catalog number	Reference
Macroolithus yaotunensis	Tangbian Formation	Hongcheng Basin, Jiangxi Province, China	NMNS CYN-2004-DINO-05-I	Wiemann et al. 2017
Macroolithus yaotunensis	Hugang Formation	Liquanqiao Basin, Henan Province, China	STIPB-E131	Wiemann et al. 2017
Macroolithus yaotunensis	Pingling Formation	Nanxiong Basin, Guangdong Province, China	STIPB-E66	Wiemann et al. 2017
Triprismatoolithus stephensi	Lower portion of the Upper Cretaceous (Campanian) Two Medicine Formation	Dave and Joel Site, Sevenmile Hill outcrops, Teton County, Montana	MOR ES101	Jackson and Varricchio 2010
Gallus gallus	-	Bonn, Germany	-	-
Crocodylus porosus	-	Taichung, Taiwan	uncatalogued specimen in NMNS	-
Tomistoma schlegelii	-	Taichung, Taiwan	uncatalogued specimen in NMNS	-